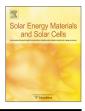


Solar Energy Materials & Solar Cells



journal homepage: www.elsevier.com/locate/solmat

Silicon nanocrystals embedded in silicon carbide as a wide-band gap photovoltaic material



J. López-Vidrier^{a,*}, P. Löper^{b,1}, M. Schnabel^b, S. Hernández^a, M. Canino^c, C. Summonte^c, S. Janz^b, B. Garrido^a

^a MIND-IN2UB, Electronics Department, University of Barcelona, Martí i Franquès 1, E-08028 Barcelona, Spain

^b Fraunhofer-Institute for Solar Energy Systems ISE, Heidenhofstr. 2, D-79110 Freiburg, Germany

^c Consiglio Nazionale delle Ricerche–Istituto per la Microelettronica e i Microsistemi (CNR-IMM), via Gobetti 101, 40129 Bologna, Italy

ARTICLE INFO

Article history: Received 13 July 2015 Received in revised form 30 September 2015 Accepted 6 October 2015

ABSTRACT

The optical and photovoltaic properties of Si NCs/SiC multilayers (MLs) are investigated using a membrane-based solar cell structure. By removing the Si substrate in the active cell area, the MLs are studied without any bulk Si substrate contribution. The occurrence is confirmed by scanning electron microscopy and light-beam induced current mapping. Optical characterization combined with simulations allows us to determine the absorption within the ML absorber layer, isolated from the other cell stack layers. The results indicate that the absorption at wavelengths longer than 800 nm is only due to the SiC matrix. The measured short-circuit current is significantly lower than that theoretically obtained from absorption within the ML absorber, which is ascribed to losses that limit carrier extraction. The origin of these losses is discussed in terms of the material regions where recombination takes place. Our results indicate that carrier extraction is most efficient from the Si NCs themselves, whereas recombination is strongest in SiC and residual a-Si domains. Together with the observed onset of the external quantum efficiency at 700–800 nm, this fact is an evidence of quantum confinement in Si NCs embedded in SiC on device level.

© 2015 Elsevier B.V. All rights reserved.

1. Introduction

The progress in material technologies together with the ambition for a substantial improvement in solar cell conversion efficiencies has led to the development of the so-called "third generation" concepts aimed at overcoming the Shockley–Queisser efficiency limit of conventional single-junction solar cells [1]. Amongst the proposed solutions, silicon nanocrystals (Si NCs) in a dielectric matrix are attractive for all-silicon tandem cells thanks to their compatibility with silicon processing combined with the possibility of tuning their band gap energy by taking advantage of the size-dependent quantum confinement [2–4]. Si NCs in SiO₂ matrix have been indeed produced using the superlattice approach [5,6], by means of which excellent NC size control and a high degree of crystallinity have been obtained [7,8]. In addition, the charge transport and the electro-optical properties of NCs embedded in such systems have been extensively studied [9–11].

However, it has been recognized that the very high band-gap energy (\approx 9 eV) of silicon oxide sets a serious bottleneck for carrier transport and, therefore, for the achievement of efficient optoelectronic devices [12]. As a consequence, recent research has targeted silicon carbide as the dielectric matrix, which provides a much lower band gap energy (\approx 2.3–2.4 eV for 3C-SiC). Aspects such as improved exciton separation and charge transport; [13–15] control of the NC size [16]; details of the precipitation and crystallization processes of Si NCs and the role of the Si/SiC interface energy on the survival of residual amorphous domains [17]; role of the Si excess in the Si-rich layers [17,18], have been recently addressed and investigated.

However, several points remain open. A crucial open point is the demonstration of quantum confinement in Si NCs when embedded in SiC matrix. Although quantum confinement in Si NCs has been demonstrated for the SiO₂ matrix [5,7], unequivocal evidence for the SiC matrix is still lacking. Band structure calculations have shown that the poorly-insulating properties of the SiC matrix are predicted to lead to inefficient quantum confinement in embedded Si NCs [19]. Moreover, the presence of a distorted transition region at the Si NC/SiC interface [17] further reduces their band gap energy [19]. Experimentally, the difficulties of detecting quantum confinement in Si NCs in SiC derive from the

^{*} Corresponding author. Tel.: + 34 93 4039175.

E-mail address: jlopezv@el.ub.edu (J. López-Vidrier).

¹ Now at: École Polytechnique Fédérale de Lausanne, Photovoltaics and Thin Film Electronics Laboratory, Rue de la Maladière 71b, CH-2002 Neuchâtel, Switzerland.

weak and broad-band photoluminescence (PL) yielded by SiC [20], which eliminates PL as a straightforward method for determining the band gap energy; and from the background absorption of the SiC matrix and of the unavoidable residual amorphous silicon [17,20], which makes it virtually impossible to study the absorption of the Si NCs independently of their surroundings.

A second crucial point is the transport mechanism in the photovoltaic (PV) device. Thermally-activated transport through the nanostructures has been demonstrated [14,15]. However, the photovoltaic properties remain very poor, which urges on an investigation of the Si NC electrical behavior at the device level. Although the PV properties of Si NC/SiC multilavers (MLs) deposited on Si surfaces were reported by different groups with different architecture [18,21], the most rigorous approach makes use of a membrane-based solar cell structure. This allows us to get rid of the contribution of absorption in the substrate, and to unambiguously attribute the electrical results to the Si NC/SiC material alone [22,23], which is not possible if the design is such that the Si substrate is in electrical contact with the rest of the device. This membrane strategy has also been employed in the field of electrolytes for dye-sensitized solar cells. In a particular study, this structure allowed achieving free-standing arrays of TiO₂ nanotubes, avoiding diffusion of carriers towards the substrate and thus improving the transport properties of the nanostructures [24]; as well, other authors succeeded in the fabrication of electrolytes containing linear polymers instead of cross-linked ones, which notably enhanced the system charge transport properties [25].

In this paper, we make use of the membrane cell structure to isolate the contribution of the Si NCs to the photovoltaic performance of Si NCs within the SiC matrix. Light-beam induced current (LBIC) mapping is used to reveal the real origin of the photocurrent signal. Moreover, we associate the spectral response of the devices to the ML material's optical properties, and show that the procedure is effective to reveal details of photogeneration and carrier collection in Si NC/SiC multilayers. Finally, the analysis demonstrates quantum confinement in Si NCs embedded in SiC at device level, and highlights the role of the overall system and its feasibility as the top junction of a tandem solar cell.

2. Experimental details

2.1. Multilayer preparation and device fabrication

Two series of MLs made up of 30 Si_{0.85}C_{0.15} (Si-rich carbide, or SRC in the following)/SiC bilayers, and pure SiC samples for reference, were deposited by plasma-enhanced chemical-vapor deposition (PECVD) on oxidized (400 nm SiO₂) c-Si (100) substrates, followed by an annealing treatment at 600 °C for 4 h plus 1100 °C for 30 min in an atmosphere of N_2 +10% O_2 . The SRC and SiC layer thicknesses (t_{SRC} and t_{SiC} , respectively) were chosen in order to obtain, after annealing, t_{SRC} equal to 3 nm (sample ML-3) and 4 nm (sample ML-4), and 5 nm for t_{SiC} in both cases. Such conditions produce a NC size equal to (4.7 ± 0.3) nm and (5+1) nm for ML-3 and ML-4 respectively [17]. Further details on ML fabrication and extensive characterization (transmission electron microscopy (TEM), X-ray diffraction, X-ray reflection, reflectance and transmittance (R&T) spectroscopy) on fully similar samples, as well as a discussion for the NC size not being equal to SRC thickness, are reported in Ref. [17]. In that reference, the multilayer structure of samples X9-3 and X9-4 is identical to that of the present samples ML-3 and ML-4, respectively. In the same reference, TEM images showed the maintenance of the ML structure for these material samples, as well as the presence of Si NCs, after the whole fabrication process. The obtained layer thicknesses out of these TEM and R&T analyzes are summarized in Table 1. A

Table 1

Summary of the active layer materials employed as the absorber layer for the membrane cell stack in the present study. The number of bilayers, SiC and SRC sublayer thicknesses evaluated by transmission electron microscopy as described in Ref. [17], ML total thickness obtained from optical simulation, and Si NC volume fraction from the different systems under study are displayed. Thickness values were obtained after annealing. The table also contains the bulk layers consisting of pure SiC (Si_{0.5}C_{0.5}), SRC with a composition of Si_{0.85}C_{0.15}, and a-Si, as well as the 4 nm multilayer, all them fabricated on fused silica substrates.

Sample	# Bilayers	t _{SiC} (nm)	t _{SRC} (nm)	Total sample thickness (nm)	Si NC volume fraction (%)
Pure SiC	-	265 ± 5	-	265 ± 5	-
ML-3	30	5 ± 1	$\textbf{3.0} \pm \textbf{0.5}$	260 ± 5	13
ML-4	30	5 ± 1	4.0 ± 0.5	290 ± 5	22
Si _{0.85} C _{0.15} ^a	-	-	-	174 ± 5	-
SiC ^a	-	-	-	68 ± 5	-
a-Si ^a	-	-	-	143 ± 5	-
X9-4 ^a	30	5 ± 1	$\textbf{4.0} \pm \textbf{0.5}$	$260\pm~5$	22

^a Deposited on fused silica substrate, for comparison of optical properties.

crystallized fraction of the Si excess in the SRC sublayer of 41% and 60% was obtained by Raman spectroscopy performed on the X9-3 and X9-4 MLs, respectively [26]. This, together with an overall excess Si volume fraction in the two multilayers of 31% and 36%, as estimated under the assumption of full demixing [17], gives a Si NC volume fraction of 13% and 22%, respectively.

To study the effect of Si NCs on the photovoltaic properties, membrane-based solar cells were fabricated with Si NC/SiC MLs, or stoichiometric SiC for reference, as absorber material. The SiC reference final thickness was 265 nm. After thermal annealing, all samples for solar cell fabrication underwent a remote hydrogen plasma treatment at 450 °C for 90 min to passivate electronic defects [22]. Table 1 summarizes the structural parameters for the different samples employed as active layers in this study. In addition to the MLs, also bulk layers with the compositions Si_{0.5}C_{0.5}, Si_{0.85}C_{0.15}, and a-Si, were prepared on fused silica substrates and used to determine the optical properties of the individual films. The a-Si material was obtained from an a-Si:H sample deposited by PECVD at 350 °C and dehydrogenated by annealing at 600 °C for 2 h. The thickness of all layers is reported in Table 1. The table also reports the parameters of the ML with 4 nm SRC on fused silica substrate (sample X9-4 in Ref. [17]), which is used as a reference for optical properties. Note the lower thickness of X9-4 with respect to ML-4 in spite of the same nominal structure, which is attributed to differences in plasma dynamics related to the different thermal and electrical properties of the substrate [17]. The n-k spectra of all reference layers were extracted from reflectance and transmittance measurements by means of optical modeling as described in [17,20].

Solar cell devices were fabricated by preparing *p-i-n* membrane-cell structures according to Ref. [22] in the configuration sketched in Fig. 1, with the NC-based material under investigation as the intrinsic (and absorber) active layer. The membrane structure allows the elimination of the c-Si wafer contribution to the PV properties of their structure. The active cell area was defined by locally removing the Si substrate and the SiO₂ insulation layer. To ensure electrical insulation, the regions outside the active cell areas were further covered by a SiO₂ layer. 20 nm thick hydrogenated *n*-type a-Si_{0.95}C_{0.05}:H and *p*-type a-Si:H layers were deposited on the rear and front sides of the structure as selective electron and hole contacts, respectively. Finally, 70 nm ITO was sputtered on both sides. After all fabrication steps, and for all measurements performed in this work, devices with an effective membrane area of $1.7\times 10^{-2}\,\text{cm}^2$ were employed. For more detailed information on the device preparation, the reader is directed to Ref. [22].

Download English Version:

https://daneshyari.com/en/article/6534958

Download Persian Version:

https://daneshyari.com/article/6534958

Daneshyari.com